Biogeosciences

Open Access

Nitrate sources and dynamics in a salinized river and estuary – a $\delta^{15}N$–NO_3^- and $\delta^{18}O$–NO_3^- isotope approach

D. Xue[1], **P. Boeckx**[3], **and Z. Wang**[1,2]

[1]Tianjin Key Laboratory of Water Resources and Environment, Tianjin Normal University, Tianjin 300387, China
[2]State Key Laboratory of Environmental Geochemistry, Institute of Geochemistry, Chinese Academy of Sciences, Guiyang 550002, China
[3]Isotope Bioscience Laboratory – ISOFYS, Faculty of Bioscience Engineering, Ghent University, Coupure links 653, 9000 Ghent, Belgium

Correspondence to: Z. Wang (wangzhongliang@vip.skleg.cn)

Abstract. To trace NO_3^- sources and assess NO_3^- dynamics in salinized rivers and estuaries, three rivers (Haihe River: HH River, Chaobaixin River: CB River and Jiyun River: JY River) and two estuaries (HH Estuary and CJ Estuary) along the Bohai Bay (China) have been selected to determine dissolved inorganic nitrogen (DIN: NH_4+, NO_2^- and NO_3^-). Upstream of the HH River, NO_3^- was removed 30.9 ± 22.1 % by denitrification, resulting from effects of the floodgate: limiting water exchange with downstream and prolonging water residence time to remove NO_3^-. Downstream of the HH River NO_3^- was removed 2.5 ± 13.3 % by NO_3^- turnover processes. Conversely, NO_3^- was increased 36.6 ± 25.2 % by external N source addition in the CB River and 34.6 ± 35.1 % by instream nitrification in the JY River. The HH and CY Estuaries behaved mostly conservatively excluding the sewage input in the CJ Estuary. Hydrodynamics in estuaries has been changed by the ongoing reclamation projects, aggravating the loss of the attenuation function of NO_3^- in the estuary.

1 Introduction

Increasing population, extensive agricultural activities and rapid development of urbanization in coastal areas have dramatically increased N loading to rivers and coastal waters (Seitzinger and Kroeze, 1998; Jennerjahn et al., 2004; Umezawa et al., 2008). Estuaries play a prominent role for delivery of terrestrially derived N to coastal water through physical, chemical and biological processes (Mulholland, 1992; Bernhardt et al., 2003; Sebilo et al., 2006; Hartzell and Jordan, 2012).

Many estuarine studies have focused on tracing N sources and assessing N dynamics in large estuarine systems, such as the Elbe Estuary (Dähnke et al., 2008) and the Atlantic coast (Middelburg and Herman, 2007) in Europe, the San Francisco Bay estuary (Wankel et al., 2006), the Mississippi River estuary (Rabalais et al.,1996), and the mid-Atlantic coast (Dafner et al., 2007) in the United States, and the Yangtze River estuary (Chai et al., 2009) and Pearl River estuary (Dai et al., 2008) in China. Compared to these large estuarine systems with high discharge of freshwater, the levels of freshwater discharge are relatively low in the small estuaries, which are characterized by salinization from seawater intrusion for rather long distances upstream (Graas and Savenije, 2008). How do these salinized estuaries respond to increased N loading? How do physical and biological processes control dissolved inorganic nitrogen (DIN: NH_4^+, NO_2^- and NO_3^-) concentration variations?

To answer these questions, an intensive study was conducted in three rivers and the corresponding estuaries characterized by different levels of salinization in a coastal municipality (Tianjin) along the Bohai Bay (China). Two investigated rivers with mean salinities around 0.5 and 0.7 flow through a rural area and converge before entering into the estuary. The third one with mean salinity around 2.2 flows through Tianjin municipality and is separated into three parts by two floodgates crossing the river, for providing water supply for the residents living along the river bank. Since the
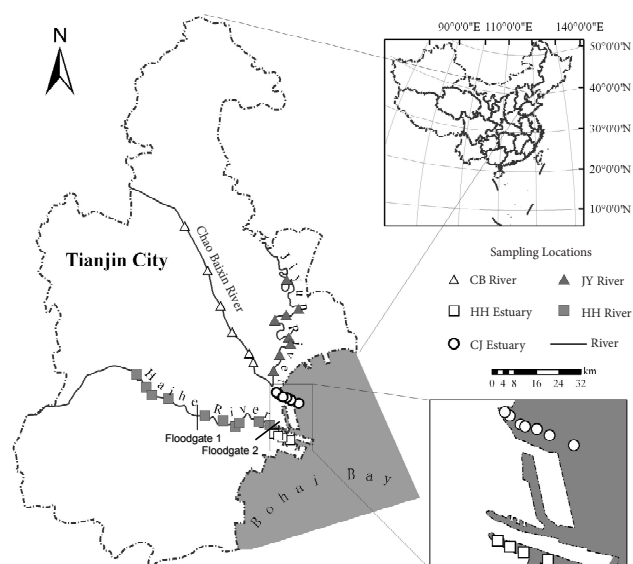
Figure 1. Sampling locations for the three investigated rivers.

rapid urbanization and population growth in Tianjin municipality, NO_3^- loading has progressively increased in rivers and estuaries associated with human activities such as agricultural runoff: untreated domestic and industrial wastewater (Gao et al., 2011). Furthermore, port construction and reclamation projects along the coastline of the municipality aggravate NO_3^- pollution (Zhang et al., 2004). Thus, tracing NO_3^- sources and assessing NO_3^- dynamics in the salinized rivers and estuaries represent fundamental goals in this study.

More than concentration data alone, the combined use of N (δ^{15}N) and O (δ^{18}O) isotopes of NO_3^- has provided a powerful tool to investigate NO_3^- dynamics and identify NO_3^- sources in estuaries (Middelburg and Nieuwenhuize, 2001; Sebilo et al., 2006; Wankel et al., 2006; Dähnke et al., 2008; Miyajima et al., 2009). Therefore, in the present study, a combined approach based on the mixing curves of DIN concentration versus salinity and δ^{15}N– and δ^{18}O–NO_3^- is applied to (1) identify potential dominant NO_3^- sources responsible for NO_3^- contamination and (2) elucidate possible NO_3^- dynamics in the different salinized rivers and the estuaries.

2 Material and method

2.1 Study area

The three rivers investigated are located in a coastal municipality, Tianjin, China (Fig. 1). The study region is influenced by a warm temperate semi-humid monsoon climate with an average annual temperature of 11.4–12.9 °C. The annual precipitation is 520–660 mm, with 75 % of the total precipitation occurring in June, July and August (Yue et al., 2010). The population of Tianjin municipality is ca. 16 million and

the density is 1100 inhabitants km^{-2}. The survey took place in the dry season on three rivers along a salinity gradient: the Haihe River (HH River) on 7 November 2012, the Chaobaixin River (CB River) on 9 November 2012 and the Jiyun River (JY River) on 10 November 2012 (Fig. 1). Water samples were also taken along the estuary of the HH River (HH Estuary) and the mixing estuary of the CB River and the JY River (CJ Estuary) on 16 November 2012 to study reactive N transformation processes from the river to the estuary (Fig. 1). The HH River is characterized by 72 km in length, ca. 100 m in width, 3–5 m in depth, and a watershed area of 2066 km^2 (Liu et al., 2001). Since the separation by the floodgate F1, the upstream part of the HH River has served as a river-type reservoir for the purpose of supplying water to the residents living along the river bank. The other floodgate F2 is located at the end of the HH River serves as flood discharging, tidal blocking and ship traffic. Although there were eight sewage outlets along the HH River, they were all forbidden to discharge. The average runoff of the HH River was 12.36×10^8 m^3 a^{-1}; the average tidal amplitude was 2.43 m; and the average flow velocity was 0.3–0.4 $m\,s^{-1}$ in 2000–2004 (Wen and Xing, 2004). The CB River flows through a rural area and is characterized by 81 km in length, ca. 700 m in width, 5–7 m in depth and a watershed area of 1387 km^2 (Gburek and Sharpley, 1998). Animal manure could be a potential dominant NO_3^- source in the CB River as this watershed is an important livestock breeding base for the municipality (Shao et al., 2010). The JY River flows through the agricultural area and is considered to be a significant water source for agricultural and domestic use. The JY River is characterized by 144 km in length, ca. 300 m in width, less than 7 m in depth and a watershed area of 2146 km^2 (Chen et al., 2000). The average runoff of the converged river mouth of the CB River and the JY River was 16.03×10^8 m^3 a^{-1}, the average tidal amplitude was 2.45 m, and the average flow velocity was 0.5–0.7 $m\,s^{-1}$ from 1990–1997 (Liang and Xing, 1999). Unfortunately, we have no hydrological data for these rivers during the study period.

2.2 Sampling and analysis

Water samples were taken on a bridge using a bucket serially from upstream downwards for the rivers and on a ship for estuarine water. The bucket was put into the river/estuary water until it reached ~ 0.5 m below the surface to sample water. Water samples were stored frozen in 1 L HDPE (high-density polyethylene) bottles for determination of physicochemical properties and δ^{15}N–NO_3^- and δ^{18}O–NO_3^-. Salinity, temperature (T), pH and dissolved oxygen (DO) were measured by a portable water quality probe (Thermo Orion, USA). Laboratory analyses included NO_3^-, NO_2^- and NH_4^+. All samples were filtered through 0.45 μm membrane filters and stored at 4 °C until analysis. Nitrate (NO_3^-), NO_2^- and NH_4^+ concentrations were analyzed on a continuous flow analyzer (Auto Analyzer 3, Seal, Germany).

The δ^{15}N– and δ^{18}O–NO_3^- values were determined by the "bacterial denitrification method" (Sigman et al., 2001; Casciotti et al., 2002; Xue et al., 2010) in the UC Davis Stable Isotope Facility of California University, which allows for the simultaneous determination of δ^{15}N and δ^{18}O of N_2O produced from the conversion of NO_3^- by denitrifying bacteria, which naturally lack N_2O–reductase activity. Isotope ratios of δ^{15}N and δ^{18}O are measured using a Thermo Finnigan GasBench + PreCon trace gas concentration system interfaced to a Thermo Scientific Delta V Plus isotope-ratio mass spectrometer (Bremen, Germany). The N_2O sample is purged from vials through a double-needle sampler into a helium carrier stream (25 mL min^{-1}) and CO_2 is removed using scrubber (Ascarite$^{®}$). By cryogenic trapping and focusing, the N_2O is compressed onto an Agilent GS-Q capillary column (30 m × 0.32 mm, 40 °C, 1.0 mL min^{-1}) and subsequently analyzed by isotope ratio mass spectrometry (IRMS).

Stable isotope data were expressed in delta (δ) units in per mil (‰) relative to the respective international standards:

$$\delta_{\text{sample}}(‰) = \left(\frac{R_{\text{sample}}}{R_{\text{standard}}} - 1 \right) \times 1000, \tag{1}$$

where R_{sample} and R_{standard} are the ^{15}N/^{14}N or ^{18}O/^{16}O ratio of the sample and standard for δ^{15}N and δ^{18}O, respectively. Values of δ^{15}N are reported relative to atmospheric air (AIR) and δ^{18}O values are reported relative to Vienna standard mean ocean water 2 (VSMOW 2). The calibration standards are the nitrates USGS 32, USGS 34 and USGS 35, and are supplied by NIST (National Institute of Standards and Technology, Gaithersburg, MD).

2.3 Mixing model

The concentration of a mixture can be calculated via a basic mixing model (Liss, 1976):

$$C_{\text{MIX}} = f \times C_R + (1 - f)C_M, \tag{2}$$

where C represents concentration; the subscripts R and M represent riverine and marine end-members, respectively; f represents the fraction of freshwater in each sample calculated from salinity (Dähnke et al., 2008):

$$f = (\text{salinity}_{\text{MAX}} - \text{salinity}_{\text{MEA}})/\text{salinity}_{\text{MAX}}, \tag{3}$$

where MAX is taken as the maximum measured salinity of marine end-member for coastal water and MEA is taken as the measured salinity of the mixture.

Isotopic values of mixed estuarine samples (δ_{MIX}) were calculated using concentration-weighted isotopic values for riverine and marine end-members, respectively (Fry, 2002; Dähnke, 2008):

$$\delta_{\text{MIX}} = [f \times C_R \times \delta_R + (1 - f)C_M \times \delta_M]/C_{\text{MIX}}, \tag{4}$$

where C represents concentration; δ represents isotopic value; the subscripts R and M represent riverine and marine end-members, respectively; and f represents the fraction of freshwater in each sample. The salinity-based isotopic mixing does not follow linear conservative mixing but shows curvilinear mixing that reflects concentration-based weighting of end-member isotopic contributions.

When a conservative mixing appears between the riverine and marine end-members, DIN distribution is expected to fall on the linear mixing line. When an enriched external source or biological transformation (e.g., mineralization, nitrification) contributes to the river, DIN distribution is expected to fall above the mixing line. In turn, when a depleted external source or the internal removal process (e.g., denitrification, assimilation) appears in the river, DIN distribution is expected to fall below the mixing line (Wankel et al., 2006). The curvilinear mixing curves of determined δ^{15}N and δ^{18}O of NO_3^- provide better information for transformation processes: an isotopic enriched NO_3^- source or internal removal processes (e.g., denitrification, assimilation) will result in a distribution of δ^{15}N and δ^{18}O falling above the mixing lines, while an isotopic depleted nitrate source or internal nitrification will result in a distribution of δ^{15}N and/or δ^{18}O falling below the mixing line.

2.4 Nitrate removal efficiency

Variation percentages of the measured NO_3^- concentrations compared to that of the calculated mixing lines were computed to assess the NO_3^- removal efficiency for the rivers and estuaries as follows:

$$\text{Variation}(\%) = \frac{C_{\text{measured}} - C_{\text{theoretical}}}{C_{\text{theoretical}}} \times 100\%, \tag{5}$$

where C_{measured} represents the measured NO_3^- concentration, and $C_{\text{theoretical}}$ represents the theoretical NO_3^- concentration calculated based on the mixing line. A variation percentage > 0 represents a source, a variation percentage < 0 represents a sink, and a variation percentage equal to 0 represents a mixing.

3 Results

3.1 Physicochemical properties

Table 1 summarizes the data of physicochemical properties collected in this study from the rivers and estuaries. Obviously, the salinities of the HH River (ranging from 0.7 to 4.9 with a mean value of 2.2) and its estuary (ranging from 18.6 to 24.1 with a mean value of 21.2) are higher than the rivers of CB (ranging from 0.5 to 0.6 with a mean value of 0.5) and JY (ranging from 0.6 to 0.8 with a mean value of 0.7) and the corresponding estuary (ranging from 2.0 to 20.0 with a mean value of 7.7). The municipality has suffered multiple seawater intrusions and regressions, which resulted in the

Table 1. Physicochemical properties and isotopic composition of NO_3^- for the three investigated rivers and the corresponding estuaries.

Location	Salinity	pH	T (°C)	DO (mg L^{-1})	NO_2^- μmol L^{-1}	NO_3^-	NH_4^+	δ^{15}N–NO_3^- ‰	δ^{18}O–NO_3^-
HH[a]	0.7	7.5	11.4	2.7	16.6	219.0	221.4	−0.2	−0.5
	0.7	7.7	12.1	4.0	18.0	145.6	332.6	0.5	0.2
	0.7	7.7	12.2	4.8	18.6	134.4	311.3	0.6	0.2
	0.8	7.9	13.2	5.0	20.8	105.0	326.9	1.1	0.5
	1.0	8.1	13.1	8.2	10.0	94.7	157.9	4.5	0.6
	2.3	8.4	12.1	10.4	7.2	90.2	124.1	4.6	1.1
	2.4	8.5	11.9	10.5	8.6	94.0	127.1	4.3	1.3
	3.7	8.3	12.7	10.4	8.8	89.0	127.3	3.9	1.2
	4.6	8.3	12.1	9.9	15.5	62.5	156.8	8.4	1.5
	4.9	8.2	11.7	9.4	14.5	70.0	149.5	7.4	1.4
Average	2.2 ± 1.7	8.1 ± 0.3	12.3 ± 0.6	7.5 ± 3.1	13.9 ± 4.8	110.4 ± 45.9	203.5 ± 87.5	3.5 ± 3.0	0.8 ± 0.7
HH[b]	18.6	8.2	10.1	10.7	6.7	25.7	88.1	8.0	5.4
	20.6	8.2	10.2	10.7	6.3	17.8	79.9	7.9	5.6
	21.3	8.1	9.6	10.7	6.2	15.1	76.9	8.1	5.7
	24.1	8.1	9.0	10.7	5.6	7.1	65.7	8.3	5.8
Average	21.2 ± 2.3	8.2 ± 0.1	9.7 ± 0.6	10.7 ± 0.0	6.2 ± 0.5	16.4 ± 7.7	77.7 ± 9.3	8.1 ± 0.2	5.6 ± 0.2
CB[a]	0.5	7.9	11.3	8.9	12.0	120.0	333.4	13.7	4.0
	0.5	8.6	10.8	10.5	7.0	134.1	167.1	14.0	4.8
	0.5	8.5	10.7	9.1	10.6	157.8	380.0	13.9	3.9
	0.5	8.5	10.5	9.9	9.9	171.5	143.9	12.2	4.3
	0.6	8.6	11.0	10.4	6.0	171.1	367.0	13.7	4.8
	0.6	8.2	10.8	10.0	8.5	152.4	210.1	14.1	5.6
Average	0.5 ± 0.1	8.4 ± 0.3	10.9 ± 0.3	9.8 ± 0.7	9.0 ± 2.3	151.2 ± 20.6	266.9 ± 105.4	13.6 ± 0.7	4.6 ± 0.6
JY[a]	0.6	8.1	9.9	7.2	7.0	40.0	72.8	6.5	0.9
	0.7	8.2	11.0	8.7	6.9	42.0	64.4	6.3	2.0
	0.7	8.2	11.3	7.5	4.4	44.0	57.6	6.4	1.4
	0.7	8.4	11.7	9.3	4.9	46.0	48.1	5.8	0.8
	0.8	8.4	12.4	9.3	4.0	76.6	12.7	5.3	1.3
	0.8	8.4	11.8	9.7	3.8	78.0	25.9	5.3	1.1
	0.8	8.5	11.8	9.9	2.2	83.3	11.1	4.4	2.8
	0.8	8.5	11.8	9.9	2.1	81.5	35.1	4.4	5.3
Average	0.7 ± 0.1	8.3 ± 0.2	11.5 ± 0.8	8.9 ± 1.1	4.4 ± 1.8	61.4 ± 19.9	41.0 ± 23.4	5.6 ± 0.8	2.0 ± 1.5
CJ[b]	2.0	8.2	7.8	10.6	7.7	153.4	328.4	13.6	5.9
	2.5	8.2	6.9	11.4	7.8	120.0	304.7	15.0	6.1
	2.7	8.3	5.7	11.5	7.6	110.0	283.3	14.7	6.4
	4.2	8.3	5.7	11.1	7.0	130.0	286.3	13.6	6.4
	9.0	8.3	5.7	11.4	5.8	37.0	180.7	11.9	6.2
	13.7	8.3	6.2	11.3	4.9	24.0	120.4	9.3	6.7
	20.0	8.2	8.6	11.2	3.4	6.1	43.2	7.1	6.9
Average	7.7 ± 6.9	8.3 ± 0.1	6.7 ± 1.2	11.2 ± 0.3	6.3 ± 1.7	82.9 ± 58.8	221.0 ± 108.0	12.2 ± 3.0	6.4 ± 0.3

[a] represents river;
[b] represents estuary.

salinization of the rivers and soil (Wang, 2004); moreover, the greater salinization level of the HH River is also related to seawater intrusion over the floodgate until upstream of the HH River for a relatively long distance. The rivers and the estuaries showed similar pH values between 7.5 and 8.6. The temperature of HH River varied around 12.3 °C, which was slightly higher than the CB River (mean is 10.9 °C) and the JY River (11.5 °C). The mean temperature of the HH Estuary (9.7) was also higher than that of the CJ Estuary (6.7). DO concentrations were relatively enriched in this study (higher than 7.2 mg L^{-1}), excluding the DO depleted area upstream of the HH River (lower than 5.0 mg L^{-1}).

3.2 DIN species

Wide concentration variations were noticeable for DIN (NH_4^+, NO_2^- and NO_3^-) species in Table 1. In the HH River, the NH_4^+ concentrations varied from 124.1 to 332.6 $\mu mol\,L^{-1}$, the NO_3^- concentrations varied from 62.5 to 219.0 $\mu mol\,L^{-1}$ and the NO_2^- concentrations varied from 7.2 to 20.8 $\mu mol\,L^{-1}$. The DIN concentrations of the HH Estuary varied smoothly (5.6–6.7 $\mu mol\,L^{-1}$ for NO_2^-, 7.1–25.7 $\mu mol\,L^{-1}$ for NO_3^- and 65.7–88.1 $\mu mol\,L^{-1}$ for NH_4^+) and were quite low compared to the HH River. Nitrate concentrations in the CB river were relatively elevated (120.0–171.5 $\mu mol\,L^{-1}$) with a continuous accumulation along the entire salinity gradient, while NO_2^- concentrations decreased from 12.0 to 6.0 $\mu mol\,L^{-1}$. Ammonium concentrations in the CB River varied from 143.9 to 380.0 $\mu mol\,L^{-1}$. The JY River also showed NO_3^- accumulation (increased from 40.0 to 83.3 $\mu mol\,L^{-1}$) along the entire salinity gradient, while a decreasing trend was observed for both NO_2^- (decreased from 7.0 to 2.1 $\mu mol\,L^{-1}$) and NH_4^+ (decreased from 72.8 to 11.1 $\mu mol\,L^{-1}$) concentrations. The CJ Estuary displayed a seaward decreasing trend with relatively elevated concentrations in NH_4^+ (328.4–43.2 $\mu mol\,L^{-1}$), NO_2^- (7.8–3.4 $\mu mol\,L^{-1}$) and NO_3^- (153.4–6.1 $\mu mol\,L^{-1}$). Compared to the other rivers and estuaries, DIN results of this study are similar to those in the Pearl River estuary (Dai et al., 2008) in South China Sea, but higher than those in the Elbe Estuary (Dähnke et al., 2008) in Europe and the San Francisco Bay estuary (Wankel et al., 2006) in the United States. The specific reasons causing such variations could potentially be linked to internal/external N source contributions and different N dynamics in the rivers and the estuaries.

3.3 Isotopic composition of NO_3^-

The isotopic composition of NO_3^- varied spatially among the rivers and the estuaries (Table 1). The $\delta^{15}N–NO_3^-$ values in the HH River varied from −0.2 to 8.4 ‰ and the $\delta^{18}O–NO_3^-$ values varied from -0.5 to 1.5 ‰. The isotopic composition of NO_3^- in the HH Estuary remained stable around 8.1 ‰ for $\delta^{15}N–NO_3^-$ and 5.6 ‰ for the $\delta^{18}O–NO_3^-$. In the CB River, the $\delta^{15}N–NO_3^-$ values were enriched with a mean of 13.6 ‰, and the $\delta^{18}O–NO_3^-$ values ranged between 3.9 and 5.6 ‰. A decrease in $\delta^{15}N–NO_3^-$ (from 6.5 to 4.4 ‰) and an increase in $\delta^{18}O–NO_3^-$ (from 0.8 to 5.3 ‰) values along the salinity were observed in the JY River. The CY Estuary demonstrated a wide range of $\delta^{15}N–NO_3^-$ (from 7.1 to 15.0 ‰) but a narrow range of $\delta^{18}O–NO_3^-$ (from 5.9 to 6.9 ‰).
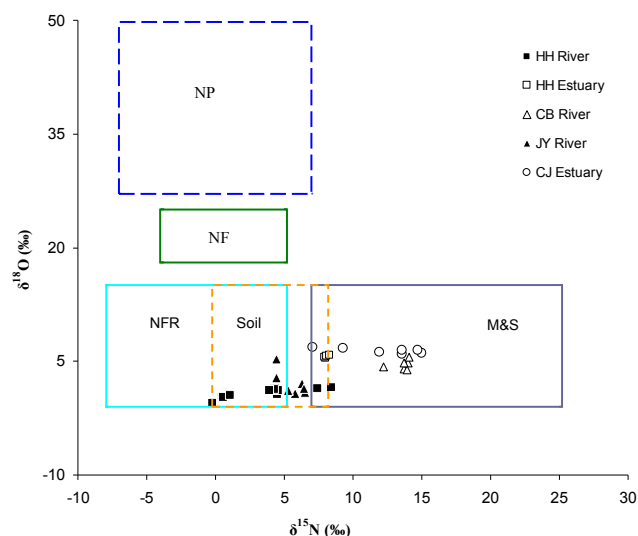

Figure 2. $\delta^{15}N–$ and $\delta^{18}O–NO_3^-$ of the salinized rivers and estuaries. Ranges of isotopic composition for five potential NO_3^- sources are adapted from Kendall et al. (2007) and Xue et al. (2009) and indicated by boxes: NO_3^- in precipitation (NP), NO_3^- fertilizer (NF), NH_4^+ in fertilizer and rain (NFR), soil N (Soil) and manure and sewage (M&S). To provide a more wide and clear range of $\delta^{18}O–NO_3^-$ values, the upper limit of NP reaches 50 ‰.

4 Discussion

4.1 Potential dominant NO_3^- sources

To derive qualitative information on the predominant NO_3^- sources in the rivers and the corresponding estuaries, a classical dual isotope approach ($\delta^{15}N–NO_3^-$ vs. $\delta^{18}O–NO_3^-$) has been applied (Fig. 2). It is clear that the isotope signatures of all the sampling locations are shown in a scattered distribution, indicating a different NO_3^- source influence in the rivers and the estuaries. Upstream of the HH River at a salinity of 1.0, a floodgate F1 separates the river into two parts, and at the end of the river at a salinity of 4.9, the other floodgate F2 controls the connection of the river to the HH Estuary. Hence, the $\delta^{15}N–$ and $\delta^{18}O–NO_3^-$ values of the HH River behaved quite differently, which moved from the overlapping area of the "NH_4^+ fertilizer" and "soil N" source boxes for the majority of the upstream sampling locations, to the overlapping area of the "soil N" and "manure and sewage" source boxes at the end of the river. In this study, the majority of the sampling locations were potentially influenced by the source of "soil N" or "sewage" not the "mineral fertilizer", as the HH River flows through the municipality without agricultural activities. In addition, it can not be excluded from the influence from saltwater intrusion from the estuary, which showed similar isotopic values to those at the end of the HH River. The distribution of the HH Estuary does not show a landward trend due to the floodgate F2 at the end of the HH River, but
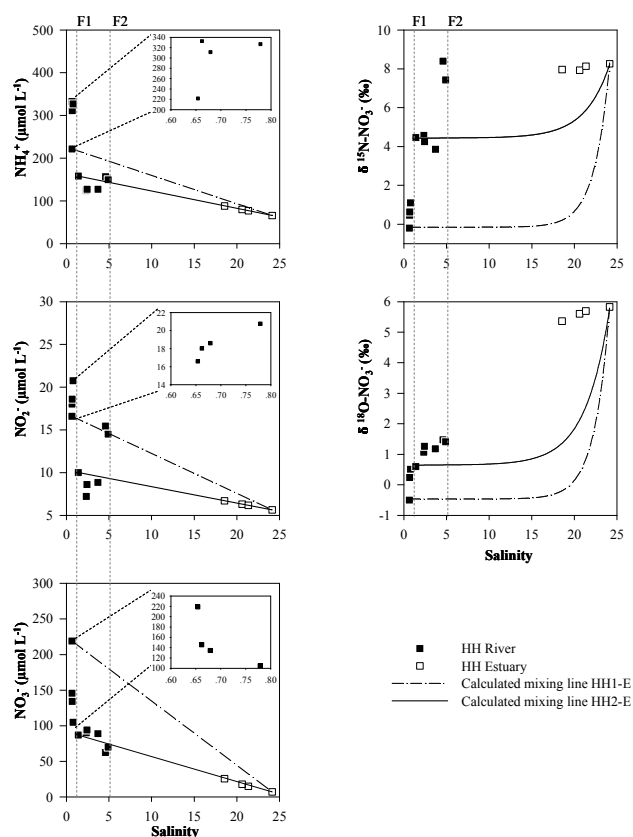
Figure 3. DIN (NH_4^+, NO_2^-, NO_3^-) concentrations and isotopic composition of NO_3^- versus salinity in the HH River and the HH Estuary. HH1-E represents the calculated mixing line between the initial upstream and the estuary; HH2-E represents the calculated mixing line between the floodgate F1 and the estuary; F represents floodgate.

falls into the range of marine NO_3^- reported by Kendall et al. (2007).

Animal manure could be a potential dominant NO_3^- source in the CB River as this watershed plays the role of an important livestock breeding base for the municipality (Shao et al., 2010). Furthermore, the $\delta^{15}N–NO_3^-$ values were enriched and varied around 14 ‰, indicating anthropogenic NO_3^- derived from manure (Kendall et al., 2007; Xue et al., 2009). The isotope signatures of the JY River were mainly concentrated in the "soil N" source box. The $\delta^{15}N–NO_3^-$ and $\delta^{18}O–NO_3^-$ values of the CJ Estuary suggested an influence of the CB River. In addition, quite high DIN concentrations (Table 1) appeared in this estuary, due to sewage discharge of mooring ships in the vicinity of the sampling area. Thus, the influence of sewage and the CB River was considered as the dominant NO_3^- source.

4.2 Nitrate dynamics in the salinized rivers and the corresponding estuaries

### 4.2.1 Nitrate dynamics in the HH River and its estuary

A mixing line (HH1-E) was set up between the most upstream sampling location in the HH River and the most downstream sampling location in the HH Estuary (Fig. 3). After the separation of the floodgate F1, the upstream of the HH River serves as a river-type reservoir. Thus, a new mixing line (HH2-E mixing line) was re-calculated between the sampling location after the floodgate and estuarine water (Fig. 3). The salinity gradient sampled in the HH River and its estuary showed a seaward decreasing trend in DIN (NH_4^+, NO_2^- and NO_3^-) concentrations and an increasing trend in $\delta^{15}N–NO_3^-$ and $\delta^{18}O–NO_3^-$ values throughout the entire salinity gradient (Fig. 3). However, the DIN and isotopic trends did not behave conservatively, as most of the measured data deviated from the calculated mixing lines.

It is clear that in the upstream part of the HH River before the floodgate F1, NO_2^- and NH_4^+ were above (a source) while NO_3^- was below (a sink) the HH1-E mixing line. Normally, the reductive removal of NO_3^- due to denitrification and assimilation is accompanied by N and O isotope fractionations. The kinetic isotope effects are responsible for preferentially utilizing the lighter isotopes ^{14}N and ^{16}O, causing an enrichment of the heavy isotopes in the remaining NO_3^- (Mariotti et al., 1981; Mayer et al., 2002; Fukada et al., 2003). Some studies reported that a linear relationship indicating an enrichment of ^{15}N relative to ^{18}O by a factor between 0.8 and 2.0 gives evidence for denitrification (Aravenaand and Robertson, 1998; Fukada et al., 2003; Xue et al., 2009) and 1.0 for assimilation (Granger et al., 2004). In our study, the ratio of N and O isotopic enrichment is 0.8, apparently implying that the removal process of NO_3^- in this river was dominated by denitrification rather than assimilation. From another aspect, elevated NH_4^+ compared to NO_3^- will inhibit NO_3^- assimilation by phytoplankton (Dugdale and Hopkins, 1978; Dugdale and MacIsaac, 1971; Dugdale et al., 2006); thus, assimilation process is unlikely significant. The linear relation between the isotopic values and the logarithm of residual NO_3^- indicated that denitrification with constant enrichment factors ($\varepsilon = -1.8$ ‰ for $\delta^{15}N$ and $\varepsilon = -1.4$ ‰ for $\delta^{18}O$) was responsible for the increases in $\delta^{18}O$ and $\delta^{15}N$ as well. The relatively small enrichment factors were potentially linked to sedimentary denitrification, as diffusion limits the effects of fractionations in the sediments on the $\delta^{15}N–$ and $\delta^{18}O–NO_3^-$ in the overlying water column (Sebilo et al., 2003; Lehmann et al., 2004; Sigman et al., 2005). The NH_4^+ species was accumulated as a source, potentially originating from organic matter decomposition not sewage discharge, as the $\delta^{15}N–NO_3^-$ values (-0.2–1.1 ‰) were out of the sewage range. Denitrification could also be the potential process for NO_2^- accumulation in the upstream part of the HH River.

However, nitrification can not be excluded, especially at relatively low DO levels which may favor ammonium oxidizers ($NH_4^+ \rightarrow NO_2^-$) rather than nitrite oxidizers ($NO_2^- \rightarrow NO_3^-$), promoting NO_2^- accumulation (Helder and De Vries, 1998).

For the HH2-E mixing line after the floodgate F1 (Fig. 3), salinity gradient sampled in the downstream of the HH River illustrated NO_3^- turned from a source (above the HH2-E mixing line) to a sink (below the HH2-E mixing line), while NO_2^- and NH_4^+ turned from a sink (below the HH2-E mixing line) to a source (above the HH2-E mixing line) at the end of the river. Nitrate accumulation may be linked to an in-stream nitrification process, in which NO_2^- and NH_4^+ were consumed to produce NO_3^-. In nitrification, the conversion of NH_4^+ to NO_2^- and NO_3^- is accompanied by marked N isotope fractionation effects, resulting in ^{15}N-depleted NO_3^- (Delwiche and Steyn, 1970; Mariotti et al., 1981; Macko and Ostrom, 1994). For $\delta^{18}O$–NO_3^- values, NO_3^- produced by nitrification in aquatic environments usually takes similar $\delta^{18}O$ values to the ambient water (Casciotti et al., 2002; Sigman et al.2005). There is evidence that O can exchange between H_2O and intermediate compounds of nitrification (Andersson et al., 1982; DiSpirito and Hooper, 1986; Kool et al., 2007). Since the $\delta^{18}O$ of estuarine water is expected to be higher than that of river water (Miyajima et al., 2009), $\delta^{18}O$–NO_3^- should increase along the salinity gradient when in situ nitrification is occurring. Thus, a decrease in $\delta^{15}N$– (4.6–3.9 ‰) and an increase in $\delta^{18}O$–NO_3^- (0.6–1.2 ‰) occurred downstream of the HH River and confirmed the in-stream nitrification process as a NO_3^- source. The NH_4^+ concentrations increased at the end of the HH River (a maximum turbidity zone), probably from the release of particle-bound NH_4^+ (Seitzinger et al., 1991; Schlarbaum et al., 2010). Results (Kranck, 1984; Eisma, 1986; Schlarbaum et al., 2010) have been reported that this NH_4^+ could originate from the mineralization of ^{15}N-enriched DON adsorbed onto the particles and was released with the estuarine turbidity maximum. The ^{15}N-enriched NH_4^+ was further converted to ^{15}N-enriched NO_3^-. Thus, the $\delta^{15}N$–NO_3^- increased sharply from 3.9 to 8.4 ‰ while the $\delta^{18}O$–NO_3^- only increased slightly from 1.2 to 1.5 ‰, resulting from taking similar $\delta^{18}O$ values to the ambient water. Another possible cause for a sharp increase in NH_4^+ concentration could be sewage discharge. Sewage is enriched in ^{15}N relative to other N sources, as ammonia volatilization causes a large enrichment of ^{15}N in the residual NH_4^+. This NH_4^+ is subsequently converted into ^{15}N-enriched NO_3^-. When salinity achieves 5, nitrifying bacterial was potentially inhibited and reduced the conversion rate from NO_2^- to NO_3^- (Pollice et al., 2002). Hence, the NO_2^- was accumulated and NO_3^- was declined in this zone.

The DIN concentrations and $\delta^{15}N$– and $\delta^{18}O$–NO_3^- in the coastal water behaved conservatively with regards to mixing. Since the separation of the floodgate F2 at the end of the HH River, the salinity has demonstrated a sudden increase from
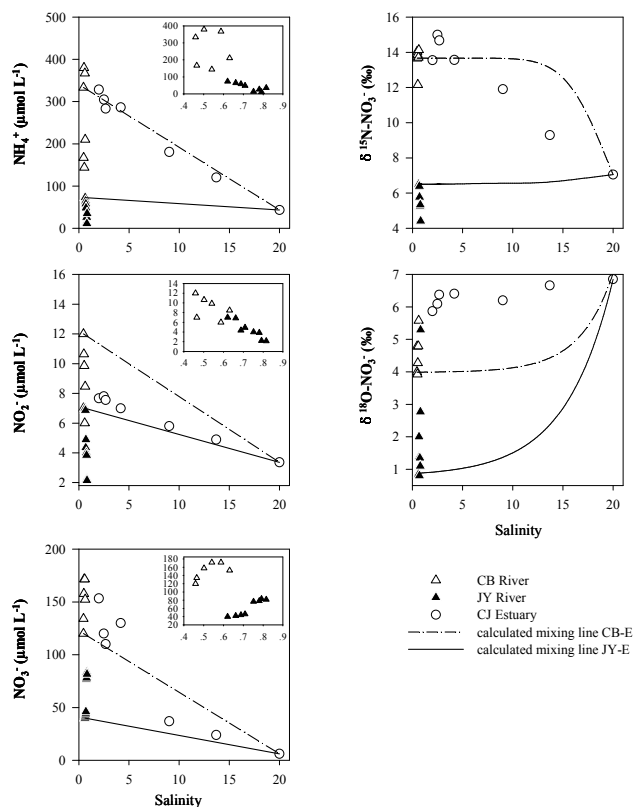
Figure 4. DIN (NH_4^+, NO_2^-, NO_3^-) concentrations and isotopic composition of NO_3^- versus salinity in the CB River, the JY River and the CJ Estuary. CB-E represented the calculated mixing line between the CB River and the CJ Estuary; JY-E represented the calculated mixing line between the JY River and the CJ Estuary.

4.9 (before the floodgate) to 18.6 (after the floodgate) in 1 km, potentially indicating that the HH river discharge was limited due to the floodgate F2. The $\delta^{15}N$–NO_3^- value of the last sampling location in the HH River was close to that of the estuarine water; hence $\delta^{15}N$–NO_3^- values remained stable at ~ 8.0 ‰. The $\delta^{18}O$–NO_3^- values increase seaward because of the high percentage of coastal water.

4.3 Nitrate dynamics in the CB River and JY River and their estuary

Compared to the HH River, the salinity of the CB and JY rivers varied in a relatively small range, from 0.5 to 0.6 for the CB River and from 0.6 to 0.8 for the JY River. Mixing lines were calculated between the CB and JY rivers and the estuarine water, respectively (Fig. 4). Both CB and JY rivers demonstrated a NO_3^- source along the salinity gradient, indicating a NO_3^- input from either in-stream nitrification or external loading.

Nitrate concentrations in the CB River were elevated with a continuous accumulation along the river. The CB River flows through a rural area with intensive livestock

production, likely resulting in NO_3^- contamination in the CB River (Shao et al., 2010). Furthermore, a regular source–sink pattern was observed for NH_4^+ concentrations while a decrease for NO_2^-. The sharp increase in NH_4^+ concentrations was probably linked to manure discharge in the rural area. The added NH_4^+ was then rapidly oxidized to NO_2^- and NO_3^- during nitrification. Hence, $\delta^{15}N$–NO_3^- values were enriched and varied around 13.6 ‰, indicating NO_3^- derived from manure (Kendall et al., 2007; Xue et al., 2009). As NO_3^- from these origins is produced via nitrification, its $\delta^{18}O$ values would not be very different from ambient water. Thus, the gradual increase in $\delta^{18}O$–NO_3^- values along the salinity gradient above the respected mixing line confirmed the in situ nitrification (see the discussion above). Thus, in the CB River, the NO_3^- turnover is mainly regulated by nitrification from external livestock N loadings.

The JY River became a significant source for NO_3^- in concert with a sink for NO_2^- and NH_4^+ species. The accumulation of NO_3^- was linked to the in-stream nitrification, resulting from the consumption of NO_2^- and NH_4^+. Evidence for this may be indicated by decreasing $\delta^{15}N$–NO_3^- and increasing $\delta^{18}O$–NO_3^- values along the river.

The salinity gradient sampled in the corresponding estuary showed a seaward decreasing trend in NH_4^+, NO_2^- and NO_3^- concentrations. The measured data in the CJ Estuary were expected to fall between the two calculated mixing lines generated from the rivers of CB and JY, because they both discharge into the same estuary. A major DIN source (above the two calculated mixing lines) appeared in the salinity zone between 2.0 and 4.2. This was probably from sewage discharge of mooring ships in the vicinity of the sampling area. The typically high $\delta^{15}N$–NO_3^- (13.6 to 15.0 ‰) values confirmed NO_3^- derivation from sewage. This point-source contamination was diluted by the estuarine water when salinity higher than 4.2, where the DIN concentrations and $\delta^{15}N$–NO_3^- values fall between the two mixing lines. The $\delta^{18}O$–NO_3^- values of the estuarine water were quite close to the $\delta^{18}O$–NO_3^- derived from the nitrification of sewage; thus, $\delta^{18}O$-NO_3^- values were expected to remain stable.

4.4 Nitrate removal efficiency in the rivers and the estuaries

In this study, most of the measured data deviated from the calculated mixing lines, indicating rivers and estuaries becoming either a source or a sink. Thus, variation percentages of the measured data compared to the calculated mixing lines were computed to assess the NO_3^- removal efficiency for the rivers and estuaries (Fig. 5). Interestingly, in the upstream part of the HH River before the floodgate F1, NO_3^- was removed 30.9 ± 22.1 % compared to the calculated mixing line. Denitrification could be the dominant NO_3^- removal process. This potentially results from the separation of the floodgate F1 which limited water exchange with downstream
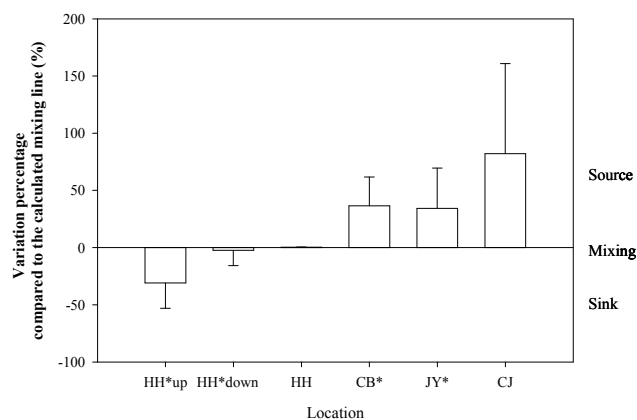
Figure 5. Variation percentage compared to the calculated mixing lines for the HH River, CB River, JY River and their corresponding estuaries of HH and CJ. The percentage > 0 represents a source, the percentage < 0 represents a sink, the percentage equal to 0 represents a mixing, and * represents a river.

water enriched in DO. Furthermore, the floodgate F1 might prolong water residence time in the upstream part to remove a significant part of riverine N loading. The downstream part of the HH River between floodgate F1 and floodgate F2 showed an extremely weak NO_3^- removal tendency (remove 2.5 ± 13.3 % of NO_3^-) from active NO_3^- turnover processes and the HH Estuary demonstrated a conservative behavior with respect to NO_3^-. In contrast, a significant source of NO_3^- is present in the CB (36.6 ± 25.2 %) and JY (34.6 ± 35.1 %) rivers compared to the calculated mixing line, explained by external N source addition and in-stream nitrification, respectively. Moreover, the CJ Estuary demonstrated higher NO_3^- accumulation efficiency (82.1 ± 78.8 %) as a result of an external N source input. Great variation percentages were observed between the sampling points from the same river or estuary, possibly resulting from different N dynamics and/or external source input.

Estuaries of rivers are considered as active sites of massive NO_3^- losses (Brion et al., 2004; Seitzinger et al., 2006), removing up to 50 % of NO_3^- (OsparCom, 2000). However, our data do not support this view as in the HH and the CJ Estuary. First, DO concentrations were higher than $10 \, mg \, L^{-1}$ not favorable for a water column NO_3^- removal processes. Second, dredging and diking work to deepen the ship channel decreased the sediment area (where denitrification mainly occurred) that is in contact with the overlying water column in the rivers (Dähnke et al., 2008); thus the NO_3^- removal ability was reduced. Third, water residence time is not long enough to remove N loads in the estuaries by NO_3^- removing processes as reclamation projects for the regional and national economy leading to the hydrodynamics of circulation in Tianjin section disappearance (Qin et al., 2012). This phenomenon could reduce water residence time and force NO_3^- pollutants moving to the northern part of Bohai Bay,

aggravating NO_3^- contamination. Furthermore, this wintertime situation, with water temperature around $10\,^\circ$C, ruled out most biological activity, and conservative mixing behavior in the HH River estuary was not overly surprising. However, the CJ Estuary became a NO_3^- source, linking to sewage discharge of mooring ships.

5 Conclusions

The combined use of salinity, DIN concentrations and NO_3^- isotopic composition revealed NO_3^- sources and dynamics in the salinized rivers of HH, CB and JY and elucidated mixing patterns of NO_3^- in the corresponding estuarine system. The HH River demonstrated a significant NO_3^- sink appeared in the upstream part of the HH River by denitrification process. This potentially results from the separation of the floodgate F1 which limited water exchange with downstream water enriched in DO and prolonged water residence time in the upstream to remove a significant part of riverine N loading. The downstream of the HH River showed an extremely weak NO_3^- removal tendency from active NO_3^- turnover processes. In contrast, a significant source of NO_3^- is present in the rivers of CB and JY, linking to external N source addition and in-stream nitrification, respectively. We found that the estuarine mixing behavior is mostly conservative excluding the point source input that appeared in the CJ Estuary. Data indicate that the rivers and their corresponding estuaries have lost their natural capacity of NO_3^- removal but turned into a significant source of NO_3^- for the adjacent Bohai Bay.

References

Andersson, K. K., Philson, S. B., and Hooper, A. B.: [18]O isotope shift in 15N NMR analysis of biological N-oxidations: H_2O-NO_2-exchange in the ammonia-oxidizing bacterium Nitrosomonas, P. Natl. Acad. Sci. USA, 79, 5871–5875, 1982.

Aravena, R. and Robertson, W. D.: Use of multiple isotope tracers to evaluate denitrification in ground water: study of nitrate from a large-flux septic system plume, Ground Water 36, 975–982, 1998.

Bernhardt, E. S., Likens, G. E., Buso, D. C., and Driscoll, C. T.: Instream uptake dampens effects of major forest disturbance on watershed nitrogen export, P. Natl. Acad. Sci. USA, 100, 10304–10308, 2003.

Brion, N., Baeyens, W., De Galan, S., Elskens, M., and Laane, R.: The North Sea: source or sink for nitrogen and phosphorus to the Atlantic Ocean?, Biogeochemistry, 68, 277–296, 2004.

Casciotti, K. L., Sigman, D. M., Galanter Hastings, M., Böhlke, J. K., and Hilkert, A. A.: Measurement of the oxygen isotopic composition of nitrate in seawater and freshwater using the denitrifier method, Anal. Chem., 74, 4905–4912, 2002.

Chai, C., Yu, Z. M., Shen, Z. L., Song, X., Cao, X., and Yao, Y.: Nutrient characteristics in the Yangtze River estuary and the adjacent east china sea before and after impoundment of the Three Gorges Dam, Sci. Total Environ., 407, 4687–4695, 2009.

Chen, L., Li, J., Guo, X., Fu, B., and Li, G.: Temporal and spatial characteristics of surface water quality in Jiyun River, Environ. Sci., 21, 61–64, 2000 (in Chinese with English abstract).

Dafner, E. V., Mallin, M. A., Souza, J. J., Wells, H. A., and Parsons, D. C.: Nitrogen and phosphorus species in the coastal and shelf waters of Southeastern North Carolina, Mid-Atlantic US coast, Mar. Chem., 103, 289–303, 2007.

Dähnke K., Bahlman, E., and Emeis, K.: A nitrate sink in estuaries? An assessment by means of stable nitrate isotopes in the Elbe estuary, Limnol. Oceanogr., 53, 1504–1511, 2008.

Dai, M., Wang, L., Guo, X., Zhai, W., Li, Q., He, B., and Kao, S.-J.: Nitrification and inorganic nitrogen distribution in a large perturbed river/estuarine system: the Pearl River Estuary, China, Biogeosciences, 5, 1227–1244, doi:10.5194/bg-5-1227-2008, 2008.

Delwiche, C. and Steyn, P.: Nitrogen isotope fractionation in soils and microbial reactions, Environ. Sci. Technol., 4, 929–935, 1970.

DiSpirito, A. A. and Hooper, A. B.: Oxygen exchange between nitrate molecules during nitrite oxidation by Nitrobacter, Biol. Chem., 261, 10534–10537, 1986.

Dugdale, R. C. and Hopkins, T. S.: Predicting the structure and dynamics of a pollution-driven marine ecosystem embedded in an oligotrophic sea, Thalassia Jugoslavica, 14, 107–126, 1978.

Dugdale, R. C. and MacIsaac, J. J.: A computational model for the uptake of nitrate in the Peru upwelling region, Invest. Pesq., 35, 299–308, 1971.

Dugdale, R. C., Wilkerson, F. P., Marchi, A., and Hogue, V.: Nutrient controls on new production in the Bodega Bay, California, coastal upwelling plume, Deep-Sea Res. Pt. II, 53, 3049–3062, 2006.

Eisma, D.: Flocculation and de-flocculation of suspended matter in estuaries, Neth. J. Sea Res., 20, 183–199, 1986.

Fry, B.: Conservative mixing of stable isotopes across estuarine salinity gradients: a conceptual framework for monitoring watershed influences on downstream fisheries production, Estuaries, 25, 264–271, 2002.

Fukada, T., Hiscock, K. M., Dennis, P. F., and Grischek, T.: A dual isotope approach to identify denitrification in ground water at a river bank infiltration site, Water Res. 37, 3070–3078, 2003.

Gao, X., Meng, H., and Yi, X.: Analysis of nitrogen pollution characteristics in water bodies of Tianjin, China Water & Wastewater, 27, 51–55, 2011 (in Chinese with English abstract).

Gburek, W. J. and Sharpley, A. N.: Hydrology control on phosphorus loss from upland agricultural watersheds, J. Environ. Qual., 270, 253–272, 1998.

Graas, S. and Savenije, H. H. G.: Salt intrusion in the Pungue estuary, Mozambique: effect of sand banks as a natural temporary

salt intrusion barrier, Hydrol. Earth Syst. Sci. Discuss., 5, 2523–2542, 2008,
http://www.hydrol-earth-syst-sci-discuss.net/5/2523/2008/.

Granger, J., Sigman, D. M., Needoba, J. A., Harrison, P. J.: Coupled nitrogen and oxygen isotope fractionation of nitrate during assimilation by cultures of marine phytoplankton, Limnol. Oceanogr. 49, 1763–1773, 2004.

Hartzell, J. L. and Jordan, T. E.: Shifts in the relative availability of phosphorus and nitrogen along estuarine salinity gradients, Biogeochemistry, 107, 489–500, 2012.

Helder, W. and De Vries, R. T. P.: Estuarine nitrite maxima and nitrifying bacteria (Ems-Dollard estuary), Netherlands J. Sea Res., 17, 1–18, 1983.

Jennerjahn, T. C., Ittekkot, V., Klöpper, S., Adi, S., Nugroho, S. P., Sudiana, N., Yusmal, A., Prihartanto, and Gaye-Haake. B.: Biogeochemistry of a tropical river affected by human activities in its catchment: brantas river estuary and coastal waters of Madura Strait, Java, Indonesia, Estuar. Coast. Shelf S., 60, 503–514, 2004.

Kendall, C., Elliott, E. M., and Wankel, S. D.: Tracing anthropogenic inputs of nitrogen to ecosystems. in: Stable Isotopes in Ecology and Environmental Science, edited by: Michener, R. and Lajtha, K., Blackwell, Maiden, 375–449, 2007.

Kool, D. M., Wrage, N., Oenema, O., Dolfing, J., and Van Groenigen, J. W.: Oxygen exchange between (de)nitrification intermediates and H_2O and its implication for source determination of NO_3^- and N_2O: a review, Rapid Commun. Mass Sp., 21, 3659–3578, 2007.

Kranck, K.: Role of flocculation in the filtering of particulate matter in estuaries, in: The Estuary as a Filter, edited by: Kennedy, V. S., New York, Academic Press, Orlando FL., 159–175, 1984.

Lehmann, M. F., Sigman, D. M., and Berelson, W. M.: Coupling the $^{15}N/^{14}N$ and $^{18}O/^{16}O$ of nitrate as a constraint on benthic nitrogen cycling, Mar. Chem., 88, 1–20, 2004.

Liang, Y. and Xing, H.: Preliminary analysis of the characteristics of tidal dynamic and sediment at the Yongdingxinhe River Mouth, Haihe Water Resources 2, 13–15, 1999. (in Chinese)

Liss, P. S.: Conservative and non-conservative behavior of dissolved constituents during estuarine mixing, in: Estuarine Chemistry, edited by: Burton, J. D. and Liss, J. D., Academic press, 93–130, 1976.

Liu, G., Fu, B., and Yang, P.: Quality of aquatic environment at Haihe River and the pollutant fluxes flowing into sea, Environ. Sci., 22, 46–50, 2001 (in Chinese with English Abstract).

Macko, S. A. and Ostrom, N. E.: Molecular and pollution studies using stable isotope. in: Stable Isotopes in Ecology and Environmental Science, edited by: Lajtha, K. and Michner, R., Blackwell Scientific, Oxford, UK, 45–62, 1994.

Mariotti, A., Germon, J. C., Hubert, P., Kaiser, P., Letolle, R., Tardieux, A., and Tardieux, P.: Experimental determination of nitrogen kinetic isotope fractionation: some principle illustration for the denitrification and nitrification processes, Plant Soil, 62, 413–430, 1981.

Mayer, B., Boyer, E. W., Goodale, C., Jaworski, N. A., Breemen, N. V., Howarth, R. W., Seitzinger, S., Billen, G., Lajtha, K., Nadelhoffer, K., Dam, D. V., Hetling, L. J., Nosal, M., and Paustian, K.: Sources of nitrate in rivers draining sixteen watersheds in the northeastern U.S.: Isotopic constraints, Biogeochemistry, 57/58, 171–197, 2002.

Middelburg, J. J. and Herman, P. M. J.: Organic matter processing in tidal estuaries, Mar. Chem., 106, 127–147, 2007.

Middelburg, J. J. and Nieuwenhuize, J.: Nitrogen isotope tracing of dissolved nitrogen behavior in tidal estuaries, Estuar. Coast. Shelf S., 53, 385–391, 2001.

Miyajima, T., Yoshimizu, C., Tsuboi, Y., Tanaka, Y., Tayasu, I., Nagata, T., and Koike, I.: Longitudinal distribution of nitrate $\delta^{15}N$ and $\delta^{18}O$ in two contrasting tropical rivers: implications for instream nitrogen cycling, Biogeochemistry, 95, 243–260, 2009.

Mulholland, P. J.: Regualtion of nutrient concentrations in a temperate forest stream: roles of upland, riparian, and instream processes, Limnol. Oceanogr., 37, 1512–1526, 1992.

OSPARCOM: Quality Status Report 2000, Region II – Greater North Sea, OSPAR Commission, 136+xiii pp., 2000.

Pollice, A., Tandoi, V., and Lestingi, C.: Influence of aeration and sludge retention time on ammonium oxidation to nitrite and nitrate, Water Res., 36, 2541–2546, 2002.

Qin, Y., Zhange, L., Zheng, B., Cao, W., Liu, X., and Jia, J.: Impact of shoreline changes on the costal water quality of Bohai Bay (2003–2011), Acta Scientiae Circumstantiae, 32, 2149–2159, 2012 (in Chinese with English Abstract).

Rabalais, N. N., Turner, R. E., Justiæ, D., Dortch, Q., Wiseman, W. J., and Sen Gupta, B. K.: Nutrient changes in the Mississippi River and system responses on the adjacent continental shelf, Estuaries, 19, 386–407, 1996.

Schlarbaum, T., Daehnke, K., and Emeis, K.: Turnover of combined dissolved organic nitrogen and ammonium in the Elbe estuary/NW Europe: results of nitrogen isotope investigations, Mar. Chem., 119, 91–107, 2010.

Sebilo, M., Billen, G., Grably, M., and Mariotti, A.: Isotopic composition of nitrate-nitrogen as a marker of riparian and benthic denitri?cation at the scale of the whole Seine River system, Biogeochemistry 63, 35–51, 2003.

Sebilo, M., Billen, G., Mayer, B., Billiou, D., Grably, M., Garnier, J., and Mariotti, A.: Assessing nitrification and denitrification in the Seine River and Estuary using chemical isotopic techniques, Ecosystems, 9, 564–577, 2006.

Seitzinger, S. P., Gardner, W. S., and Spratt, A. K.: The effect of salinity on ammonia sorption in aquatic sediments: implications for benthic nutrient recycling, Estuaries, 2, 167–174, 1991.

Seitzinger, S. P., Harrison, J. A., Böhlke, J. K., Bouwman, A. F., Lowrance, R., Peterson, B., Tobias, C., and Van Drecht, G.: Denitrification across landscapes and waterscapes: a synthesis, Ecol. Appl., 16, 2064–2090, 2006.

Seitzinger, S. P. and Kroeze, C.: Global distribution of nitrous oxide production and N inputs in freshwater and coastal marine ecosystems, Glob. Biogeochem. Cycles, 12, 93–113, 1998.

Shao, X., Deng, X., Yuan, X., and Jiang, W.: Identification of potential sensitive areas of non- point source pollution in downstream watershed of Chaobaixin River, Environ. Sci. Surv., 29, 37–41, 2010 (in Chinese with English abstract).

Sigman, D. M., Casciotti, K. L., Andreani, M., Barford, C., Galanter, M., and Böhlke, J. K.: A bacterial method for the nitrogen isotopic analysis of nitrate in seawater and freshwater, Anal. Chem., 73, 4145–4153, 2001.

Sigman, D. M., Granger, J., DiFiore, P. J., Lehmann, M. M., Ho, R., Cane, G., and van Geen, A.: Coupled nitrogen and oxygen isotope measurements of nitrate along the eastern

North Pacific margin, Global Biogeochem. Cy., 19, GB4022, doi:10.1029/2005GB002458, 2005.

Umezawa, Y., Hosono, T., Onodera, S., Siringan F., Buapeng, S., Delinom, R., Yoshimizu, C., Tayasu, I., Nagata, T., and Taniguchi, M.: Sources of nitrate and ammonium contamination in groundwater under developing Asian megacities, Sci. Total. Environ., 404, 361–376, 2008.

Wang, L.: A discussion on the deep fresh water salinization in the plain region of Tianjin City, Geol. Surv. Res., 27, 169–176, 2004 (in Chinese with English Abstract).

Wankel, S. D., Kendall, C., Francis, C. A., and Paytan, A.: Nitrogen sources and cycling in the San Francisco Bay Estuary: a nitrate dual isotopic composition approach, Limnol. Oceanogr., 51, 1654–1664, 2006.

Wen, S. and Xing, H.: The characteristics of water and sand in the Haihe River estuary and movement rule analysis, Haihe Water Resources 2, 28–31, 2004. (in Chinese)

Xue, D., Botte, J., De Baets, B., Accoe, F., Nestler, A., Taylor, P., Van Cleemput, O., Berglund, M., and Boeckx, P.: Present limitations and future prospects of stable isotope methods for nitrate source identification in surface- and groundwater, Water Res., 43, 1159–1170, 2009.

Xue, D., De Baets, B., Vermeulen, J., Botte, J., Van Cleemput, O., and Boeckx, P.: Error assessment of nitrogen and oxygen isotope ratios of nitrate as determined via the bacterial denitrification method, Rapid Commun. Mass Sp., 24, 1979–1984, 2010.

Yue, F., Liu, X., Li, J., Zhu, Z., and Wang, Z.: Using nitrogen isotopic approach to identify nitrate sources in waters of Tianjin, China. Bull. Environ, Contam. Toxicol. 85, 562–567, 2010.

Zhang, J., Yu, Z. G., Raabe, T., Liu, S., Starke, A., Zou, L., Gao, H., and Brockmann, U.: Dynamaics of inorganic nutrient species in the Bohai seawaters, J. Marine Syst., 44, 189–212, 2004.